Critical quantum fluctuations in the degenerate parametric oscillator

P. D. Drummond,[1] K. Dechoum,[1] and S. Chaturvedi[2]

[1]*Department of Physics, University of Queensland, St. Lucia 4067, Queensland, Australia*
[2]*School of Physics, University of Hyderabad, Hyderabad 500046, India*

We develop a systematic theory of critical quantum fluctuations in the driven parametric oscillator. Our analytic results agree well with stochastic numerical simulations. We also compare the results obtained in the positive-P representation, as a fully quantum-mechanical calculation, with the truncated Wigner phase-space equation, also known as the semiclassical theory. We show when these results agree and differ in calculations taken beyond the linearized approximation. We find that the optimal broadband noise reduction occurs just above threshold. In this region where there are large quantum fluctuations in the conjugate variance and macroscopic quantum superposition states might be expected, we find that the quantum predictions correspond very closely to the semiclassical theory.

I. INTRODUCTION

In a companion paper [1], we treated the below-threshold nonlinear squeezing in a driven quantum parametric oscillator. In the present paper, we turn to the problem of the critical fluctuations at threshold, where the previous perturbation theory, as well as diagrammatic techniques, all give divergent results. We find that the use of an appropriately rescaled asymptotic perturbation method, using the fundamental cubic stochastic process as the zeroth-order term, gives a well-behaved analytic theory. The results are in complete agreement with numerical simulations in the positive-P representation. In addition, the results also agree with the previous nonlinear perturbation theory in an overlap region just below threshold. This allows us to obtain analytic predictions to complement numerical simulations, both below and inside the region of strong critical fluctuations at the threshold for down-conversion—where quantum squeezing is at its largest.

The theory of linear quantum squeezing in the parametric oscillator is well developed, both in theory [2–11] and in experiment [12,13], in the region below threshold. However, the usual theory is linearized, and therefore diverges in the interesting critical region. Methods including nonlinear corrections often use many-body Feynman-diagram techniques [7,8] to extend the linear theory [9–11]. These have the drawback that they involve infinite sets of diagrams and are difficult to use systematically at the critical point. This type of problem is common in nonequilibrium quantum physics. It represents a fundamental drawback in the Feynman-diagram approach, in which both the coupling to reservoirs and the nonlinear terms are treated as perturbations. Other methods involving number-state expansions—like direct solutions of the master equation, or the stochastic Schrödinger equation—are inapplicable to these large Hilbert spaces, and are usually insoluble from an analytic approach. We also note that since this is a nonequilibrium system, it presents an example of a quantum phase transition in which the usual canonical-ensemble techniques are simply inapplicable.

We treat these questions using the positive-P representation [14], combined with two matched expansion techniques, one valid below the critical point, and one valid at the critical point. These methods agree in the overlap region below threshold. Results are also verified by the use of direct numerical stochastic-equation simulations, which are valid in all regions. In the present paper, we focus on the critical squeezing results. The broadband squeezing obtained by considering quadrature moments is optimized in a region of large critical fluctuations just above threshold, rather than below threshold where we found [1] the optimum narrow-band quantum squeezing in the spectrum.

We also compare the above results with a semiclassical approach, that is, a truncated Wigner phase-space equation. This equation corresponds to a classical theory with added vacuum fluctuations. A comparison between the positive-P representation (fully quantum-mechanical) and semiclassical theories permits us to see how far one can go and what is the limitation of this extended classical point of view. At the critical point, fluctuations are large, and the system may be thought to display the characteristics of a macroscopic quantum superposition state (Schrödinger cat), as it undergoes quantum transitions between the two possible classical phases of the subharmonic field. We emphasize here that the steady-state density matrix is expected to be a mixed state, as it is an open system. If there is any Schrödinger-cat-like behavior, it would be related to a transient or conditional measurement, such as the squeezing spectrum itself.

There is a fundamental problem with any system used to investigate macroscopic superpositions. In order to show that any nonclassical "paradox" occurs, one must demonstrate that all hidden-variable explanations can be ruled out. Surprisingly, the semiclassical theory—which is fully realistic—works extremely well in this region. Our conclusion is that for this system, any macroscopic quantum superposition that may occur in the transient dynamics cannot be readily distinguished from classical realism.

II. HAMILTONIAN AND MASTER EQUATION

The model considered here is the degenerate parametric oscillator and is described in detail elsewhere [1]. For completeness, we repeat the definitions of the Hamiltonian here.

The system of interest is an idealized interferometer, which is resonant at two frequencies, ω_1 and $\omega_2 = 2\omega_1$. It is externally driven at the larger of the two frequencies. Both frequencies are damped due to cavity losses. Down-conversion of the pump photons to resonant subharmonic-mode photons occurs due to a $\chi^{(2)}$ nonlinearity present inside the cavity. The Heisenberg-picture Hamiltonian that describes this open system [2] is

$$\hat{H} = \hat{H}_0 + \hat{H}_{int} + \sum_{j=1,2} \hbar(\hat{a}_j \hat{\Gamma}_j^\dagger + \hat{a}_j^\dagger \hat{\Gamma}_j) + \hat{H}_R. \quad (2.1)$$

An interaction picture is obtained with the definition that free evolution is given by

$$\hat{H}_0 = \sum_{j=1,2} \hbar \omega_j \hat{a}_j^\dagger \hat{a}_j.$$

In the case of resonant down-conversion, with just a second harmonic, the interaction Hamiltonian is

$$\hat{H}_{int}/\hbar = i\mathcal{E}[\hat{a}_2 - \hat{a}_2^\dagger] + \frac{i\chi}{2}[\hat{a}_2 \hat{a}_1^{\dagger 2} - \hat{a}_2^\dagger \hat{a}_1^2]. \quad (2.2)$$

Here $\hat{a}_1, \hat{a}_2$ represent the fundamental and second-harmonic modes, respectively, while $\mathcal{E}$ is proportional to the coherent input or driving field at the second-harmonic frequency, assumed to be at exact resonance with the cavity mode. Using standard techniques [15] to eliminate the heat bath, we obtain the following master equation for the reduced density operator of the system in the interaction picture:

$$\frac{\partial \hat{\rho}}{\partial t} = \frac{1}{i\hbar}[\hat{H}_{int}, \hat{\rho}] + \gamma_1(2\hat{a}_1 \hat{\rho} \hat{a}_1^\dagger - \hat{a}_1^\dagger \hat{a}_1 \hat{\rho} - \hat{\rho} \hat{a}_1^\dagger \hat{a}_1)$$
$$+ \gamma_2(2\hat{a}_2 \hat{\rho} \hat{a}_2^\dagger - \hat{a}_2^\dagger \hat{a}_2 \hat{\rho} - \hat{\rho} \hat{a}_2^\dagger \hat{a}_2), \quad (2.3)$$

where γ_i are the internal-mode amplitude-damping rates.

In the classical limit, the system has the well-known classical equations of intracavity parametric oscillation,

$$\frac{d\alpha_1}{dt} = [-\gamma_1 \alpha_1 + \chi \alpha_1^* \alpha_2],$$

$$\frac{d\alpha_2}{dt} = \left[-\gamma_2 \alpha_2 + \mathcal{E} - \frac{1}{2}\chi \alpha_1^2\right]. \quad (2.4)$$

These equations are valid in the limit of large photon number. There is a phase transition at the critical driving field of $\mathcal{E} = \mathcal{E}_c = \gamma_1 \gamma_2/\chi$, corresponding to an intracavity photon number of $N_c = \gamma_1^2/\chi^2$. For driving fields below this value, one has

$$\alpha_1 = 0,$$

$$\alpha_2 = \mathcal{E}/\gamma_2, \quad (2.5)$$

while for fields above this value, the signal field α_1 is bistable, with

$$\alpha_1 = \pm \sqrt{\frac{2}{\chi}(\mathcal{E} - \mathcal{E}_c)},$$

$$\alpha_2 = \frac{\gamma_1}{\chi}. \quad (2.6)$$

It is the behavior in the critical region that we are most interested in as the usual linearized methods break down. Just above the critical region, we see that the quantum system has some of the character of a Schrödinger "cat." There are two possible values for the subharmonic amplitude α_1, and the system prior to detection may be in a transient superposition state of these amplitudes. This situation has been analyzed previously for the case of a rapidly decaying second-harmonic field [16,17]. Here we investigate it for a general case. We consider the question from the viewpoint of asking what signature of the observables of the system would entitle one to claim that a Schrödinger cat or macroscopic superposition, was responsible.

A. The positive-P representation

In order to treat quantum evolution, we now turn to the methods of operator representation theory, as described previously [1]. We consider two types of representation — the normally ordered positive-P representation and the semiclassical truncated Wigner method. The positive-P representation equations are used to treat the full quantum evolution, without any truncation of higher-order derivatives in the Fokker-Planck equation. Given appropriate assumptions about vanishing boundary terms (valid for $\chi \ll \gamma_j$), the following stochastic equations are obtained, for any driving field $\mathcal{E}$:

$$d\alpha_1 = [-\gamma_1 \alpha_1 + \chi \alpha_1^+ \alpha_2]dt + \sqrt{\chi \alpha_2}\,dw_1(t),$$

$$d\alpha_1^+ = [-\gamma_1 \alpha_1^+ + \chi \alpha_1 \alpha_2^+]dt + \sqrt{\chi \alpha_2^+}\,dw_2(t),$$

$$d\alpha_2 = \left[-\gamma_2 \alpha_2 + \mathcal{E} - \frac{1}{2}\chi \alpha_1^2\right]dt,$$

$$d\alpha_2^+ = \left[-\gamma_2 \alpha_2^+ + \mathcal{E} - \frac{1}{2}\chi \alpha_1^{+2}\right]dt. \quad (2.7)$$

The nonvanishing stochastic correlations are given by

$$\langle dw_k(t)\rangle = 0,$$

$$\langle dw_k(t)dw_l(t)\rangle = \delta_{kl}dt. \quad (2.8)$$

This means that $dw_k(t)$ represent two real Gaussian, uncorrelated stochastic processes, so that the amplitude of the stochastic fluctuations that act on the signal mode are dependent on the pump-field dynamics through the term $\sqrt{\chi \alpha_2}$.

B. The semiclassical theory

We can also write a c-number phase-space equation using an approximate form of the Wigner representation [18],

which is equivalent to stochastic electrodynamics. This can be mapped into the following stochastic differential coupled equations:

$$d\alpha_1 = [-\gamma_1 \alpha_1 + \chi \alpha_1^* \alpha_2] dt + \sqrt{\gamma_1} dw_1(t),$$

$$d\alpha_1^* = [-\gamma_1 \alpha_1^* + \chi \alpha_1 \alpha_2^*] dt + \sqrt{\gamma_1} dw_1^*(t),$$

$$d\alpha_2 = \left[-\gamma_2 \alpha_2 - \frac{\chi}{2} \alpha_1^2 + \mathcal{E} \right] dt + \sqrt{\gamma_2} dw_2(t),$$

$$d\alpha_2^* = \left[-\gamma_2 \alpha_2^* - \frac{\chi}{2} \alpha_1^{*2} + \mathcal{E} \right] dt + \sqrt{\gamma_2} dw_2^*(t). \quad (2.9)$$

Here $dw_k(t)$ is now a *complex* Gaussian white noise whose mean and variance are given by

$$\langle dw_k(t) \rangle = 0,$$

$$\langle dw_k(t) dw_l^*(t) \rangle = \delta_{kl} dt. \quad (2.10)$$

The above equation is identical to the equation derived in positive-P representation when one discards the noise terms; both methods reproduce the well-known classical equations in this limit.

C. Observable moments and spectra

The details of how observable moments and spectra are calculated in the positive-P stochastic method and the Wigner representation are given in the previous paper [1]. The technique for treating external-field spectra was introduced by Yurke [3], and by Collett and Gardiner [4].

These external-field measurements are obtained from the input-output relations of

$$\hat{\Phi}_j^{out}(t) = \sqrt{2\gamma_j^{out}} \, \hat{a}_j(t) - \hat{\Phi}_j^{in}(t), \quad (2.11)$$

where $\hat{\Phi}_j^{in}(t)$ and $\hat{\Phi}_j^{out}(t)$ are the input and output photon fields, respectively, evaluated at the output-coupling mirror. The most efficient transport of squeezing is obtained if we assume that all the signal losses occur through the output coupler, so that $\gamma_1 = \gamma_1^{out}$. We will assume this to be the case.

The quadrature variables of the system have the definitions

$$\hat{x}_j = (\hat{a}_j + \hat{a}_j^\dagger),$$

$$\hat{y}_j = \frac{1}{i} (\hat{a}_j - \hat{a}_j^\dagger). \quad (2.12)$$

There are also corresponding external-quadrature-field variables, defined as

$$\hat{X}_j = (\hat{\Phi}_j^{out} + \hat{\Phi}_j^{out\dagger}),$$

$$\hat{Y}_j = \frac{1}{i} (\hat{\Phi}_j^{out} - \hat{\Phi}_j^{out\dagger}). \quad (2.13)$$

Similarly, we can define c-number stochastic quadrature variables within the relevant representations, thus giving

$$x_j = (\alpha_j + \alpha_j^+),$$

$$y_j = \frac{1}{i} (\alpha_j - \alpha_j^+). \quad (2.14)$$

Of most interest here is $\hat{y}_1$ since this is the low-noise, squeezed quadrature; the instantaneous correlation functions of the intracavity field operators are called the moments. The fundamental property of the positive-P representation is that the ensemble average of any polynomial of the random variable a and a^* exactly corresponds to the Hilbert-space expectation of the corresponding normally ordered product of the annihilation and creation operators. The fundamental property of the Wigner function is that the ensemble average of any polynomial weighted by the Wigner density corresponds (approximately, for the truncated Wigner case) to the expectation of the corresponding symmetrized product of the annihilation and creation operators. Therefore, the truncated theory with a positive Wigner function can be viewed as equivalent to a local realistic hidden-variable theory, since one can obtain quadrature fluctuation predictions by following an essentially classical prescription.

III. SCALED EQUATIONS: POSITIVE-P REPRESENTATION

In order to avoid the divergences of the previous method at the critical point of this system where $\mathcal{E} = \mathcal{E}_c$, we define new scaled quadrature variables and use a different expansion [19] valid inside the critical region of $|\mu - 1| = |\mathcal{E}/\mathcal{E}_c - 1| < \sqrt{g}$, where g is a dimensionless coupling constant (typically $g \ll 1$) defined by

$$g = \frac{\chi}{\sqrt{2\gamma_1 \gamma_2}}.$$

The new pump-mode variable x_2^c now corresponds to the real scaled depletion in the pump-mode amplitude, relative to the undepleted value at the critical point. The signal-mode variable x_1^c now describes the critical fluctuation amplitude scaled to be of order 1 at threshold, while y_1^c is simply defined as y_1. The definitions are

$$x_1^c = \sqrt{g} x_1,$$

$$y_1^c = y_1,$$

$$x_2^c = \frac{1}{g} \left[\frac{\chi x_2}{\gamma_1} - 2 \right],$$

$$y_2^c = \sqrt{\frac{2\gamma_r}{g}} y_2. \quad (3.1)$$

It is convenient to also define a new scaled time and driving field as

$$\eta = \frac{\mu-1}{g} = \frac{1}{g}\left[\frac{\mathcal{E}}{\mathcal{E}_c}-1\right],$$

$$\tau = \gamma_1 g t. \qquad (3.2)$$

The parameter η is a measure of how close the driving field is to its value at the bifurcation threshold, scaled in terms of the coupling constant so that the critical region of large fluctuations is defined by $|\eta| < 1$. The time has now been scaled both by the decay rate in the signal mode γ_1 and the parameter g.

In the case of the positive-P representation, the equations in the new variables are functions of the dimensionless parameters g, η, and $\gamma_r = \gamma_2/\gamma_1$,

$$dx_1^c = \frac{1}{2}[x_1^c x_2^c + g y_1^c y_2^c]d\tau + \sqrt{2}dw_{xc},$$

$$g dy_1^c = -\left[2y_1^c + \frac{g}{2}(x_2^c y_1^c - y_2^c x_1^c)\right]d\tau - i\sqrt{2g}dw_{yc},$$

$$g dx_2^c = \gamma_r[2\eta - x_2^c - (x_1^c - g y_1^{c2})/2]d\tau,$$

$$g dy_2^c = -\gamma_r[y_2^c + x_1^c y_1^c]d\tau. \qquad (3.3)$$

The Gaussian white-noise increments dw_{ic} $(i=x,y)$ are not independent, and have the following properties:

$$\langle dw_{ic}\rangle = 0,$$

$$\langle dw_{xc}^2\rangle = \langle dw_{yc}^2\rangle = \langle 1 + g x_2/2\rangle d\tau,$$

$$\langle dw_{yc}dw_{xc}\rangle = g^{3/2}\langle y_2\rangle d\tau. \qquad (3.4)$$

We can develop an asymptotic theory in the small-g limit for the critical region, just as easily as below threshold. The result is a simple theory that correctly predicts the scaling of the critical and squeezing fluctuations, as well as making close predictions of their size for finite g. It is important to note here the presence of the $\sqrt{g}dw_{yc}$ term in these equations. This scaling factor of $\sqrt{g}$, is added to ensure that the fluctuations in this variable occur up to an order equivalent to that of other mean values. This simplifies the procedure of truncating the deterministic and noise terms to a given order.

The approximation we use here entails expanding the stochastic trajectories in an asymptotic series in g, and solving the resulting equations on a term-by-term basis. This entails a power-series expansion similar to the one used below threshold, except with new variables

$$x_j^c = \sum_{n=0}^{\infty} g^n x_j^{(n)},$$

$$y_j^c = \sum_{n=0}^{\infty} g^n y_j^{(n)}.$$

The first set of equations are

$$dx_1^{(0)} = \frac{1}{2}x_1^{(0)}x_2^{(0)}d\tau + \sqrt{2}dw_{xc}^{(0)},$$

$$g dy_1^{(0)} = -2y_1^{(0)}d\tau + \sqrt{2g}dw_{yc}^{(0)},$$

$$g dx_2^{(0)} = \gamma_r(2\eta - x_2^{(0)} - [x_1^{(0)}]^2/2)d\tau,$$

$$g dy_2^{(0)} = -\gamma_r(y_2^{(0)} + x_1^{(0)}y_1^{(0)})d\tau. \qquad (3.5)$$

The Gaussian white-noise increments $dw_{xc}^{(0)}$, $dw_{yc}^{(0)}$ have the variance

$$\langle\langle\langle[dw_{xc}^{(0)}]^2\rangle\rangle\rangle = \langle\langle\langle[dw_{yc}^{(0)}]^2\rangle\rangle\rangle = d\tau.$$

A significant point about these equations is that in the squeezed quadrature, the $y_1^{(0)}$ solution can be worked out without reference to any of the other variables, and it gives zero noise in the external quadrature at zero frequency. Of course, couplings between the variables will emerge to higher orders in the expansion, and this generates the actual critical fluctuations in the squeezed quadrature. Also, the $y_2^{(0)}$ variable is simply driven by the other fields and can be obtained as soon as the other fields are known.

A. Critical fluctuations

We now consider what happens at or near the classical threshold of $\eta = 0$. In a model where the second-harmonic generation does not cause the pump mode to deplete, we would have $x_2^{(0)} = 2\eta$, and at threshold the critical fluctuations in x_1 would diffuse outward without any bound. When depletion is included, the critical fluctuations in the quadrature x_1 are finite, but very slowly varying compared to those in the other variables. The pump field can therefore be adiabatically eliminated to first order in the expansion.

Near threshold ($g\eta \ll 1$) the decay term in the unsqueezed quadrature x_1 is roughly $-x_2$, which is of order 1. The pump mode will be depleted, so obviously x_2 must be negative in order for this to be stable. The scaled pump-field decay is γ_r/g, and the squeezed-quadrature decay is of order $1/g$. If γ_r is much larger than g, it is possible to adiabatically eliminate both the pump amplitude and the squeezed quadrature in the equations for the large critical fluctuations x_1. Since we are taking the limit of small g, we shall assume that this is possible to zeroth order in the asymptotic expansion. In the adiabatic elimination, we must solve for the steady-state values of the pump x_2, given an instantaneous first-order critical fluctuation x_1. To leading (zeroth) order this gives, where $x = x_1^{(0)}$,

$$x_2^{(0)} = 2\eta - x^2/2. \qquad (3.6)$$

Substituting in the equation for x_1, we find that

$$dx = (\eta x - x^3/4)d\tau + \sqrt{2}dw_{xc}. \qquad (3.7)$$

This equation is a standard form of the stochastic equation [20], which is the real cubic process often found at a critical point, even for thermal equilibrium systems. The solution for the distribution of x is given by

$$P(x) = \exp(\eta x^2/2 - x^4/16).$$

The steady-state critical variance in x_1 is given to zeroth order by

$$\langle x_1^2 \rangle^{(0)} = \langle x^2 \rangle = \frac{\int x^2 dx \exp(\eta x^2/2 - x^4/16)}{\int dx \exp(\eta x^2/2 - x^4/16)}. \qquad (3.8)$$

The variance of the critical fluctuations at the critical point, $\eta = 0$, is therefore given to lowest order by the variance of a cubic process, which is a ratio of Γ functions,

$$\langle x_1^2 \rangle^{(0)} = \frac{4\Gamma(3/4)}{\Gamma(1/4)} = 1.3520 \ldots \qquad (3.9)$$

In a normally ordered representation, the normally ordered version of the quadrature variance operator differs by 1 from its symmetric form. However, to this order in the calculation, corrections of this size can be neglected. This is an example of much more general results on representation invariance [21] of the large fluctuations that occur near critical points. In general, these have a behavior to leading order that is rather classical, and does not depend on the operator ordering. Using this, we find the steady state of the unsqueezed quadrature at threshold. Denoting the symmetric expectation value by the subscript S, to leading order we get (at the critical point)

$$\langle \hat{x}_1^2 \rangle_S = \frac{1}{g} \langle x^2 \rangle = \frac{4\Gamma(3/4)}{g\Gamma(1/4)}.$$

This variable has the critical slowing down expected at threshold, that is, the unsqueezed signal quadrature is the one in which the critical fluctuations occur. The value for the size of the critical fluctuations can be used to calculate the depletion of the scaled pump-mode amplitude x_2. Using Eqs. (3.2) and (3.8), to first order in g it is

$$x_2^{(0)} = 2\eta - \langle x^2 \rangle/2. \qquad (3.10)$$

The size of the depletion is consistent with an $N^{-1/2}$ conversion efficiency for pump photons to signal photons at the critical point. In summary, by using the fact that a cubic stochastic equation has a potential solution, the quadrature moments can be obtained for any driving field in the critical region [20].

B. Critical squeezing in positive-P representation

We can now find the steady-state variance of the squeezed quadrature at threshold. Because the fluctuations in the squeezed quadrature are very small, we must work to higher order in the asymptotic expansion to obtain a nontrivial result. To achieve this, it is most useful to introduce equations in the higher-order moments y_1^2 and $z_1 = x_1 y_1$. The corresponding stochastic equations are derived using Ito rules for variable changes, so that

$$g d(y_1^2) = -2\left[1 + 2y_1^2 + \frac{1}{2}g(x_2 + x_2 y_1^2 - y_2 z_1)\right] d\tau$$
$$+ 2\sqrt{g} y_1 dw_{yc},$$

$$g dz_1 = \left[-2z_1 + \frac{g}{2}y_2(-x_1^2 + gy_1^2 + 2g)\right] d\tau + \sqrt{g} x_1 dw_{yc}$$
$$+ gy_1 dw_{xc}. \qquad (3.11)$$

The squeezing variance at threshold from Eq. (3.11) is obtained by taking expectation values. At the steady state, $\langle d(y_1^2) \rangle = 0$. In addition, the expectation value of any noise term is always zero in an Ito equation, so that

$$\langle y_1^2 \rangle^{(1)} = -\frac{g}{4}\langle (1 + y_1^2)x_2 - y_2 z_1 \rangle^{(0)}. \qquad (3.12)$$

The expectation value of the correlation between y_1 and any x_i variable is trivial to zeroth order, as these must factorize. Thus, we can write immediately

$$\langle (1 + y_1^2)x_2 \rangle^{(0)} = \langle 1 + y_1^2 \rangle^{(0)} \langle x_2 \rangle^{(0)} = \eta - \langle x^2 \rangle/4. \qquad (3.13)$$

However, the expectation value of correlations between y_2 and z_1 does not factorize. We first must obtain the equation for this correlation. To lowest order this is

$$g d(y_2 z_1) = -[2y_2 + \gamma_r(y_2 + z_1)]z_1 d\tau + (\text{noise}).$$

The noise correlations do not matter, since we can immediately take expectation values and obtain

$$\langle y_2 z_1 \rangle^{(0)} = \frac{-\gamma_r}{2 + \gamma_r}\langle z_1^2 \rangle^{(0)} = \frac{\gamma_r}{4 + 2\gamma_r}\langle x^2 \rangle.$$

To obtain this result we have once again used the factorization properties of the y_1 fluctuations to zeroth order. Combining the above results together, we find that the steady-state variance of the squeezed quadrature up to first order in g is

$$\langle :\hat{y}_1^2: \rangle = -\frac{1}{2} - \frac{g\eta}{4} + \frac{g}{16}\left(\frac{2 + 3\gamma_r}{2 + \gamma_r}\right)\langle x^2 \rangle. \qquad (3.14)$$

This is plotted in Fig. 1, along with the predictions obtained from the nonlinear corrections to the usual below-threshold theory [1]. It can be seen that both theories agree in an overlap region where $1 - \mu \simeq \sqrt{g}$. For $|1 - \mu| < g$ so that $|\eta| < 1$, the below-threshold theory diverges, and the critical expansion is needed to obtain correct results.

The intracavity squeezing moment for a model with a nondepleted pump mode is 1/2. Our theory predicts that a depleted parametric oscillator will get no closer to this intracavity lower limit than a term that scales as g, that is as $N^{-1/2}$. The best squeezing in the overall moment is, paradoxically, not just below, but rather just above threshold. It can be seen that in contrast to the unsqueezed quadrature, the dominant term in the decay to the steady state does not de-
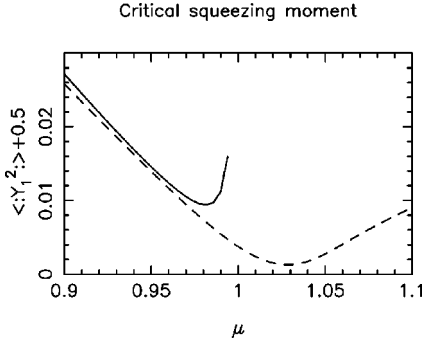
FIG. 1. Squeezing moment with $g^{-2} = 1000$, $\gamma_r = 0.5$. The solid line gives the below-threshold expansion; the dashed line gives the critical expansion.

pend on the pump-mode photon number N. This means the squeezed quadrature does not experience critical slowing down as the unsqueezed quadrature does, and has a linewidth similar to the value below threshold. In practical terms, the unsqueezed critical fluctuations would be much easier to observe, as they are the dominant effect at the critical point.

IV. SCALED EQUATIONS: SEMICLASSICAL THEORY

As in the positive-P equations, we must define new scaled-quadrature variables for the semiclassical equations, in order to avoid divergences at the critical point. We define these as previously, except for y_2^c, which now must include the large symmetrically ordered vacuum fluctuations,

$$y_2^c = \sqrt{2\gamma_r} y_2.$$

The equations in these new variables are now

$$dx_1^c = \frac{1}{2}[x_1^c x_2^c + \sqrt{g}\, y_1^c y_2^c]d\tau + \sqrt{2}\,dw_{x1}(\tau),$$

$$gdy_1^c = \left[-2y_1^c + \frac{\sqrt{g}}{2}x_1^c y_2^c - \frac{g}{2}x_2^c y_1^c\right]d\tau + \sqrt{2g}\,dw_{y1}(\tau),$$

$$gdx_2^c = \gamma_r\left[2\eta - x_2^c - \frac{1}{2}(x_1^2 - g y_1^2)\right]d\tau + 2\gamma_r\sqrt{g}\,dw_{x2}(\tau),$$

$$gdy_2^c = -\gamma_r[y_2^c + \sqrt{g}\,x_1^c y_1^c] + 2\gamma_r\sqrt{g}\,dw_{y2}(\tau), \quad (4.1)$$

where the nonvanishing moments of the noise variables are

$$\langle dw_{xj}^2\rangle = \langle dw_{yj}^2\rangle = d\tau.$$

The stochastic equations can be solved by matching the powers of g in the corresponding time-evolution equations. The zeroth-order set of equations is (discarding orders up to one in g in the right side of the above set equations)

$$dx_1^{(0)} = \frac{1}{2}x_1^{(0)}x_2^{(0)}d\tau + \sqrt{2}\,dw_{x1}(\tau),$$

$$gdy_1^{(0)} = -2y_1^{(0)}d\tau + \sqrt{2g}\,dw_{y1}(\tau),$$

$$gdx_2^{(0)} = -\gamma_r\left[2\eta - x_2^{(0)} - \frac{1}{2}(x_1^{(0)})^2\right]d\tau + 2\gamma_r\sqrt{g}\,dw_{x2}(\tau),$$

$$gdy_2^{(0)} = -\gamma_r y_2^{(0)}d\tau + 2\gamma_r\sqrt{g}\,dw_{y2}(\tau). \quad (4.2)$$

We can solve for the steady-state values of the pump x_2^c, neglecting the noise in this quadrature

$$x_2^{(0)} = 2\eta - (x_1^{(0)})^2/2; \quad (4.3)$$

substituting this expression in the equation for $x_1^0 = x$ we have

$$dx = [\eta x - x^3/4] + \sqrt{2}\,dw_{x1}(\tau). \quad (4.4)$$

This equation is the same as obtained in the positive-P case, generating the same distribution and, consequently, the same steady-state critical variance.

Critical squeezing in semiclassical theory

Following the same procedure as in the positive-P representation, we can now find the steady-state variance of the squeezed quadrature at threshold going to higher-order in the asymptotic expansion to obtain a nontrivial result. Introducing equations in the higher order moments in the new variables y_1^2 and $z_1 = x_1^c y_1^c$, the corresponding stochastic equations are

$$gd(y_1^2) = -2\left[2y_1^2 - 1 - \frac{\sqrt{g}}{2}y_2^c z_1 + \frac{g}{2}x_2^c y_1^2\right]d\tau$$
$$+ 2\sqrt{2g}\,y_1^c dw_{y1}(\tau),$$

$$gd(z_1) = \left[-2z_1 + \frac{\sqrt{g}}{2}x_1^2 y_2^c + g\sqrt{g}\,y_1^2 y_2^c\right]d\tau + \sqrt{2g}\,x_1^c dw_{y1}(\tau)$$
$$+ \sqrt{2}g y_1^c dw_{x1}(\tau). \quad (4.5)$$

The squeezing variance at threshold is obtained from the above equation taking the expectation values. At the steady state we have

$$\langle y_1^2\rangle = \frac{1}{2} + \frac{\sqrt{g}}{4}\langle y_2^c z_1\rangle - \frac{g}{4}\langle x_2^c y_1^2\rangle. \quad (4.6)$$

The expectation value of the correlation between y_1^c and x_2^c variables is trivial in zeroth order, as this must factorize. Thus we can write

$$\langle x_2^c y_1^2\rangle^{(0)} = \langle x_2^c\rangle^{(0)}\langle y_1^2\rangle^{(0)} = \eta - \langle x^2\rangle/4 \quad (4.7)$$

and then

$$\langle y_1^2\rangle = \frac{1}{2} - \frac{g\eta}{4} + \frac{g}{16}\langle x^2\rangle + \frac{\sqrt{g}}{4}\langle y_2^c z_1\rangle. \quad (4.8)$$

To obtain the correlation between y_2^c and z_1 we need to write the equation for this correlation

$$g d(y_2^c z_1) = \left\{ y_2^c \left[-2z_1 + \frac{\sqrt{g}}{2} x_1^2 y_2^c + g \sqrt{g} y_1^2 y_2^c \right] \right.$$

$$\left. + z_1 [-\gamma_r (y_2^c + \sqrt{g} z_1)] \right\} d\tau + \sqrt{2g} x_1^c y_2^c dw_{y1}(\tau)$$

$$+ \sqrt{2} g y_1^c y_2^c dw_{x1}(\tau) + 2 \gamma_r \sqrt{g} z_1 dw_{y2}(\tau). \quad (4.9)$$

To lowest order we get

$$\langle y_2^c z_1 \rangle^{(0)} = -\frac{\gamma_r \sqrt{g}}{2 + \gamma_r} \langle z_1^2 \rangle^{(0)} + \frac{\sqrt{g}/2}{2 + \gamma_r} \langle x_1^2 y_2^2 \rangle^{(0)}. \quad (4.10)$$

Combining the above results together, we find the steady-state variance of the squeezed quadrature up to first order in g

$$\langle \hat{y}_1^2 \rangle = \frac{1}{2} - \frac{g\eta}{4} + \frac{g}{16} \langle x^2 \rangle - \frac{g}{8} \left(\frac{\gamma_r}{2 + \gamma_r} \right) \langle x^2 \rangle + \frac{g}{4} \left(\frac{\gamma_r}{2 + \gamma_r} \right) \langle x^2 \rangle$$

$$= \frac{1}{2} - \frac{g\eta}{4} + \frac{g}{16} \left(\frac{2 + 3\gamma_r}{2 + \gamma_r} \right) \langle x^2 \rangle, \quad (4.11)$$

where we have used the zero-order solution $\langle y_2^2 \rangle^{(0)} = 2\gamma_r$.

This result is exactly the same as obtained in positive-P representation, giving quite confident support for the expression, up to first order in perturbation theory, of the squeezed quadrature at threshold.

V. NUMERICAL SIMULATIONS

The value of the nonlinear correction to the spectrum of the scaled internal squeezed quadrature, $S(\Omega)$, can be worked out from a full numerical simulation [22] of the relevant nonlinear stochastic equations. For the simulations, we chose values of $g^2 = 10^{-3}$, $\gamma_r = 0.5$. The simulations used a total dimensionless time interval of $\tau_{max} = 1000$. Time steps of $\Delta\tau = 0.1$ and $\Delta\tau = 0.2$ were compared to ensure convergence. The algorithmic technique is described elsewhere [23] and uses a semi-implicit central-partial-difference technique. As done previously, to obtain the small nonlinear corrections near the optimum squeezing, we simulated the difference between the linear and nonlinear forms of the stochastic equation, in order to minimize sampling errors. It was also useful to initialize the x quadratures with a Gaussian ensemble close to the known steady-state variance, in order to reduce the time taken to achieve equilibrium.

Typically, the relative error in the correlations due to finite step size was around 10^{-4} with these step sizes.

Critical squeezing

At the critical point, where $\eta = 0$, we used 10^4 trajectories, giving relative sampling errors of typically 2×10^{-2}. The calculated squeezing moment from the critical point stochastic differential equation simulations was $\langle Y_1^2 \rangle + 0.5 = 0.0038 \pm 10^{-4}$. This is in poor agreement with the below-threshold expansion, which is only applicable for $|\mu - 1| > g$. The below-threshold expansion clearly fails closer to threshold than about $\mu = 0.97$ for this value of g, and predicts

infinite fluctuations in both quadratures at the critical point. In the region where $|\mu - 1| < g$, much better agreement is naturally obtained with the critical-point expansion of the present paper, which predicts a value of $\langle Y_1^2 \rangle + 0.5 = 0.003\,75$. This agreement verifies our analytic prediction that the total squeezing, integrated over all frequencies, is actually lower at and just above threshold, than it is just below threshold where the zero-frequency squeezing is minimized.

Very similar results were obtained from the Wigner semiclassical-theory simulations, which is as expected from the predictions of the asymptotic theory.

We find that the spectral results for the squeezed quadrature resulted in a value for the zero-frequency spectrum, of $V(0) = 2.02 \times 10^{-2} \pm 0.4 \times 10^{-3}$. This is finite, but much larger than the optimum squeezing value [1] obtained below threshold. In other words, we find that the narrow-band squeezing is not as large as just below threshold—but the broadband squeezing is still improving at the threshold point, with an optimum value just above threshold.

VI. CONCLUSION

We have calculated the quantum fluctuations at the classical threshold, using a nonlinear stochastic positive-P theory, with both asymptotic approximations and a numerical technique.

At the critical point, the scaling behavior is quite different from the behavior just below threshold, and must be calculated by using an asymptotic perturbation theory, valid at the threshold itself. The total squeezing moment is actually minimized at a driving field just above threshold and scales as $N_c^{-1/2}$. This behavior was confirmed in our simulations. This apparent paradox can be attributed to the fact that the critical fluctuations mostly tend to broaden the squeezing spectrum, which has a strong effect at zero frequency, but does not diminish the total squeezing moment, which is integrated over all frequencies.

A calculation with the truncated Wigner method, or semiclassical technique, was also carried out. Well below threshold, we found in a previous paper that while the linear terms agreed with full quantum calculation, nonlinear corrections and higher-order correlations tended to disagree, especially for low second-harmonic losses. However, at the critical point, the situation changes. Here, where the dominant terms are nonlinear, we find excellent agreement between the two methods. While quantum fluctuations are indeed large at the critical point, it appears that an equally acceptable interpretation of the observed noise characteristics exists via a semiclassical model, which is essentially a type of hidden-variable theory. Above threshold, when bistability is more pronounced, previous studies have shown that the two models can be readily distinguished by their tunneling predictions, which are completely different [5].

As we have shown, in the region where incipient bistability is evident, there are large quantum fluctuations and strong squeezing. However, due to coupling with the external reservoirs, the quantum behavior can be also rather well described in a semiclassical model. This illustrates the problem of trying to identify behavior characteristic of macroscopic

superpositions, which might be thought to exist in this situation. We suggest that it is necessary to prove that no classical-like hidden-variable theory can describe the observed behavior, if we wish to ascribe any paradoxical interpretation to the observed results. Ideally, this would necessitate the demonstration of a macroscopic Bell inequality [24].

In the present case, the semiclassical description — which is essentially a hidden-variable theory — is able to accurately reproduce the quantum predictions near the critical point. Thus, it seems that there is no uniquely "catlike" behavior in the results we obtain here, at least for the parameter values employed. This is an indication of difficulties in observing Schrödinger-cat-like behavior in a physical system coupled to the outside world. Nevertheless, the present theory does give a case in which critical quantum fluctuations are soluble for a nonequilibrium phase transition, which does not have a Gibbs ensemble solution.

ACKNOWLEDGMENTS

[1] S. Chaturvedi, K. Dechoum, and P.D. Drummond, Phys. Rev. A **65**, 033805 (2002).

[2] P.D. Drummond, K.J. McNeil, and D.F. Walls, Opt. Acta **27**, 321 (1980); **28**, 211 (1981).

[3] B. Yurke, Phys. Rev. A **32**, 300 (1985).

[4] C.W. Gardiner and M.J. Collett, Phys. Rev. A **31**, 3761 (1985); M.J. Collett and D.F. Walls, *ibid.* **32**, 2887 (1985).

[5] P. Kinsler and P.D. Drummond, Phys. Rev. A **43**, 6194 (1991).

[6] P.D. Drummond and P. Kinsler, Quantum Semiclassic. Opt. **7**, 727 (1995); P. Kinsler and P.D. Drummond, Phys. Rev. A **52**, 783 (1995).

[7] J. Schwinger, J. Math. Phys. **2**, 407 (1961).

[8] L.V. Keldysh, Sov. Phys. JETP **20**, 1018 (1965).

[9] C.J. Mertens, T.A.B. Kennedy, and S. Swain, Phys. Rev. Lett. **71**, 2014 (1993); C.J. Mertens, T.A.B. Kennedy, and S. Swain, Phys. Rev. A **48**, 2374 (1993); C.J. Mertens, J.M. Hasty, H.H. Roark III, D. Nowakowski, and T.A.B. Kennedy, *ibid.* **52**, 742 (1995); C.J. Mertens and T.A.B. Kennedy, *ibid.* **53**, 3497 (1996).

[10] L.I. Plimak and D.F. Walls, Phys. Rev. A **50**, 2627 (1994).

[11] O. Veits and M. Fleischhauer, Phys. Rev. A **52**, R4344 (1995); **55**, 3059 (1997).

[12] L.A. Wu, H.J. Kimble, J.L. Hall, and H. Wu, Phys. Rev. Lett. **57**, 2520 (1986).

[13] A. Heidmann, R.J. Horowicz, S. Reynaud, E. Giacobino, C. Fabre, and G. Camy, Phys. Rev. Lett. **59**, 2555 (1987).

[14] S. Chaturvedi, P.D. Drummond, and D.F. Walls, J. Phys. A **10**, L187 (1977); P.D. Drummond and C.W. Gardiner, *ibid.* **13**, 2353 (1980).

[15] H.J. Carmichael, *Statistical Methods in Quantum Optics 1* (Springer, Berlin, 1999).

[16] M. Wolinsky and H.J. Carmichael, Phys. Rev. Lett. **60**, 1836 (1988).

[17] M.D. Reid and L. Krippner, Phys. Rev. A **47**, 552 (1993).

[18] P.D. Drummond and P. Kinsler, J. Opt. B: Quantum Semiclassical Opt. **7**, 727 (1995); S. Chaturvedi and P.D. Drummond, Phys. Rev. A **55**, 912 (1997).

[19] P. Kinsler and P.D. Drummond, Phys. Rev. A **52**, 783 (1995).

[20] S. Chaturvedi and P.D. Drummond, Eur. Phys. J. B **8**, 251 (1999).

[21] P.D. Drummond, Phys. Rev. A **33**, 4462 (1986).

[22] H.J. Carmichael, J.S. Satchell, and S. Sarkar Phys. Rev. A **34**, 3166 (1986).

[23] P.D. Drummond and I.K. Mortimer, J. Comput. Phys. **93**, 144 (1991).

[24] P.D. Drummond, Phys. Rev. Lett. **50**, 1407 (1983); A. Gilchrist, P. Deuar, and M. Reid, *ibid.* **80**, 3169 (1988).